LAND DEGRADATION & DEVELOPMENT

Land Degrad. Develop. **9**, 57–66 (1998)

DIRECT FIELD MEASUREMENT OF WIND DRAG ON VEGETATION FOR APPLICATION TO WINDBREAK DESIGN AND MODELLING

P. F. GRANT AND W. G. NICKLING*

Department of Geography, University of Guelph, Guelph, Ontario, Canada, N1G 2W1

Received 15 May 1997; Accepted 14 August 1997

ABSTRACT

A field instrument was designed and field tested for measuring the applied wind load on trees and surface-mounted obstacles in a natural boundary layer. Using this instrument, the effect of vegetation porosity on the drag coefficient of small conifer trees (h = 1·4 m) was determined directly in the field. Drag coefficients for two simple solid geometric forms (cone and cylinder) having approximately the same size (height and diameter) as the conifer trees were also measured over a relatively wide range of Reynolds numbers and the results compared to published drag curves for these shapes. The field study found that the porous element had a higher drag coefficient than a solid element, both for the solid element tested and for the drag coefficient suggested for surface-mounted solid obstacles. The drag coefficient changed on a continuum with porosity, rising initially from the value measured for the element as a solid, reaching a peak at an intermediate value and eventually falling to zero when the element was removed. This peak in the drag coefficient versus porosity curve corresponds to reports that shelterbelt efficiency peaks at medium-porosities, and is an important relationship in terms of modelling momentum extraction of vegetation, one which has not been shown previously in the literature. Findings of this study have direct application to the modelling of shelterbelts and windbreaks and the assessment of the amount of vegetation cover required to suppress wind erosion in rangeland vegetation communities.

KEY WORDS: windbreak design; wind drag on vegetation; modelling of shelterbelts; wind erosion; instrument design

INTRODUCTION

When wind, blowing across a surface, encounters large obstacles, such as isolated shrubs, trees or shelterbelts, a proportion of the wind's momentum is absorbed by the vegetation resulting in a reduction of wind speed. This wind-speed reduction proportionally decreases the available shear force to the surface thereby reducing the wind-erosion potential in the lee of the wind barrier.

Land uses, such as livestock grazing and crop production, can cause an increase in the potential for wind erosion because of the removal of natural or planted groundcover and alteration of soil structure. Management strategies to reduce wind erosion have incorporated the use of windbreaks, shelterbelts and structural barriers that result in a reduction of wind speeds in the lee. Ranging practices, particularly on marginal lands, such as in the American southwest and Australia, have been partly responsible for dust storms, causing health and traffic hazards (Hyers and Marcus, 1981). Planting or maintaining natural vegetation cover at sufficient canopy densities can eliminate the likelihood of wind erosion. Moreover, on cropped fields, the implementation of windbreaks has the added benefit of creating a favourable micro-climate that can lead to an increase in crop productivity (Heisler and DeWalle, 1988). Maximizing the benefits of windbreaks requires a thorough understanding of the physical interaction between the wind and the barrier.

*Correspondence to: W. G. Nickling, Department of Geography, University of Guelph, Guelph, Ontario, Canada N1G 2W1.

Contract grant sponsor: Natural Sciences and Engineering Research Council of Canada.

CCC 1085–3278/98/010057–10$17·50

Although much effort has gone into the measurement and characterization of wind flow in the lee of wind barriers and isolated obstacles at a range of scales, relatively little attention has been given to the direct interaction of the air with the individual plants that can be characterized by a drag coefficient. It is this interaction, at the microlevel, that is responsible for the observed down-wind flow field. In general, the work that has been carried out can be divided into two basic categories: (i) shear-stress partitioning: in which the role of vegetation in protecting the surface from erosion is determined (e.g. Marshall, 1971; Gillette and Stockton, 1989; Musick and Gillette, 1990; Stockton and Gillette, 1990; Iversen *et al*., 1991; Raupach, 1992; Raupach *et al*., 1993; Nickling and McKenna Neuman, 1995; Wolfe and Nickling, 1996), and (ii) effects of shelterbelts on wind flow and microclimatology (e.g. Hagen and Skidmore, 1971: Seginer and Sagi, 1971/1972; Seginer, 1972; Wilson, 1987). In the case of the latter, most of this work has gone into characterizing wind interaction with two-dimensional barriers and as a result 'the shelter effects and aerodynamics of two-dimensional artificial fences and screens, including the role of shelterbelt density (porosity) in determining shelter effects, are largely understood' (Wang and Takle, 1996: 83). Taylor (1988) summarized the research of porosity versus drag coefficient for two-dimensional barriers on a single curve. The drag coefficient is highest for the solid barrier and decreases on a continuum as porosity is increased (Figure 1).

Our understanding of wind interaction with three-dimensional, porous obstacles, however, such as tree windbreaks and isolated trees and shrubs, is much less complete (Heisler and DeWalle, 1988). The consequence of this lack of knowledge results in the use of surrogate data in models. For example, Raupach (1992) and Raupach, *et al*. (1993), by necessity, use drag coefficients of solid roughness elements reported by Taylor (1988) to represent natural, porous vegetation. Furthermore, the very causes of wind-speed reduction, pressure perturbation related to width and structure, permeability and drag force, are largely unknown for three-dimensional, porous obstacles (Wang and Takle, 1996).

Measurements of shelterbelt drag coefficient have been accomplished largely through calculation of the momentum deficit from the flow field surrounding the obstacle (e.g. Woodruff *et al*., 1963; Seginer and Sagi, 1971/1972; Seginer, 1972; Wang and Takle, 1995; Wang and Takle, 1996). Other attempts have been made to measure the drag coefficient by scaling down vegetation for wind-tunnel tests (Harrje *et al*., 1982; Heisler and DeWalle, 1988). Wind-tunnel studies have also measured the drag coefficient for broad leaves (Vogel, 1989), spruce shoots (Grant, 1985) and for whole trees (Mayhead, 1973).

Few studies, however, have measured directly the drag coefficient of vegetation as it relates to porosity under field conditions. As a result, this study was undertaken to measure the drag coefficient of a surface mounted tree at various porosities and wind speeds in a natural boundary layer. In addition, a simple field instrument for measuring the drag force on a tree is introduced and field tested. Data derived from this type

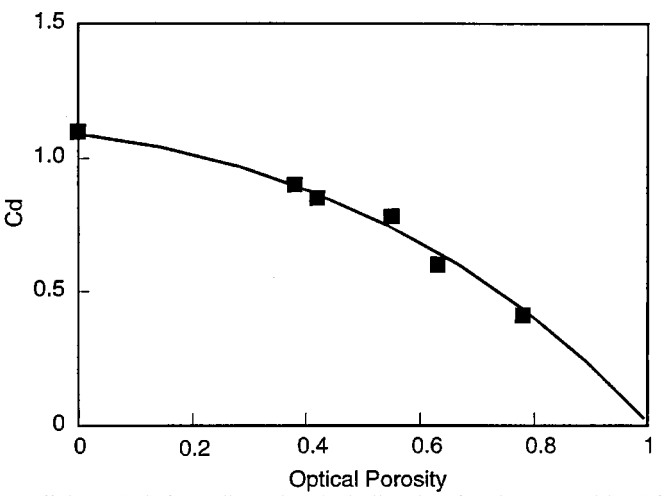

Figure 1. Drag coefficients (Cd) for 2-dimensional windbreaks of various porosities (after Taylor, 1988)

of investigation can be used directly in models dealing with wind reduction and shear-stress partition through sparse vegetation canopies (i.e. Raupach, *et al.*, 1993; Wolfe and Nickling, 1996).

STUDY LOCATION

Measurements were carried out on the eastern end of a flat, grass field (sod farm) with the longest fetch (700 m) facing into the prevailing westerly winds. The study site was bounded by a small hedgerow 20 m in the lee, a road 300 m to the south with another open field across the road, the barn and office 300 m to the SW, a hedgerow 700 m to the west and a row of trees 200 m to the north. Wind data collected from 190° to 310° azimuth were used in the analysis.

Surface conditions throughout the duration of the study were held at a near-constant with clipping of the grass to a height of approximately 0·05 m, twice weekly. Within the instrument area the grass was cut with a hand mower, as the large machinery could not be navigated around the instruments.

THE EXPERIMENTAL TREE

A number of factors, such as flexibility, leaf density or porosity, wind speed and vegetation structure, affect the drag coefficients of natural roughness elements, such as trees and shrubs (Grant, 1985). Initially, live shrubs or small trees were to be used in the field experiment. However, as the goal of this empirical study was to couple drag coefficient with element porosity, all other parameters needed to be held constant and therefore an artificial tree was selected.

The tree used for this study was a commercially available artificial scots pine Christmas tree. This type of tree had several advantages:

(1) The branches could be added and removed quite simply to make changes in porosity. Moreover, by assigning specific positions for each of the branches at a given porosity, if insufficient data were collected at one porosity, the exact tree porosity and structure could be reconstructed for further measurements.
(2) By reproducing the same tree structure and using the same tree for each porosity, the multitude of potential complicating factors was controlled and the effect of porosity isolated.
(3) The rigid branches and needles resisted bending and realignment under the force of the wind, thereby reducing the problem of a changing porosity due to deformation during high-speed winds.

The total drag exerted on vegetation is related to the flow through and around the plant which is largely controlled by the porosity. Measurements of both two- and three-dimensional porosity were made for three selected tree configurations. Two-dimensional optical porosity was measured by taking black and white photographs of the shrub with a white sheet as a backdrop. Optical porosity was determined using a digital analyser and JAVA software (Wolfe, 1993). Use of this system allows for an unbiased determination of the amount of black (element) and white (pore space) in the photograph. However, much of the small-scale porosity, such as between the needles, is likely beyond the resolution of the analysis. Measures of three-dimensional or volumetric porosity were taken using a simple water displacement technique. The volume of the tree was estimated as if it were non-porous, by creating an imaginary outer perimeter. Then the tree was dismantled, the individual branches submerged into a water-filled graduated cylinder, and the individual branch volumes summed and the porosity calculated. In order to expel air bubbles from the branches, a surfactant in the form of liquid detergent was added to the water (Brand, 1987).

Numerous studies have measured the drag coefficients for surface-mounted, solid elements (e.g. cones, pyramids, hemispheres and cubes) in wind tunnels and flumes. To investigate the sensitivity and precision of the drag meter, a cone of approximately the same size of the tree ($h = 1{\cdot}45$ m; base $= 1{\cdot}0$ m) and a cylinder ($h = 1{\cdot}45$ m; $d = 0{\cdot}30$ m) were constructed of styrofoam and a cardboard cylinder respectively. The drag coefficients of these elements were measured for comparison with the tree and with published data for solid objects in free stream flow.

INSTRUMENTATION AND DATA ACQUISITION

To determine the drag coefficient (C_d) of a surface-mounted obstacle, the wind speed (u), the fluid density (ρ), the cross-sectional area (A) and the drag force (F) must be known:

$$C_d = \frac{2F}{\rho A u^2} \tag{1}$$

The variables u, ρ, and A can be measured directly. In contrast, F must be measured directly or determined with a knowledge of the obstacle's C_d. For simple geometric shapes, C_d can be obtained from established drag curves. Few data, however, are readily available for more complex geometric forms and in particular those with porous configurations which may change with increasing wind speed.

Field Measurement of Drag

A field instrument capable of measuring the drag on the tree was developed to satisfy the following criteria: (i) it must be strong enough to support the weight of the tree or shrub, (ii) sensitive to changes in applied load with small, rapid changes in wind speed and (iii) allow for alignment into the wind as wind direction changes.

Initially, the field instrument was to be designed with a buried section consisting of a vertical lever arm with a central fulcrum. However, as Mayhead (1973) found, a vertical lever arm, with the force distributed across it, necessitates the determination of the centre of pressure across the arm. In a boundary layer, the centre of force is difficult to determine even for simple geometric shapes, becoming very complex for irregular elements such as trees or shrubs. Under free-stream conditions, Grant (1985) was able to use the centre of mass as the load point. Knowing that the wind speed increases proportional to the logarithm of height above the surface, this assumption would not hold true for a surface-mounted, roughness element.

The field instrument design is shown in Figure 2. The entire unit was buried to just below the point where the four support arms are attached to the sides. A roughness element was mounted in the sleeve and secured

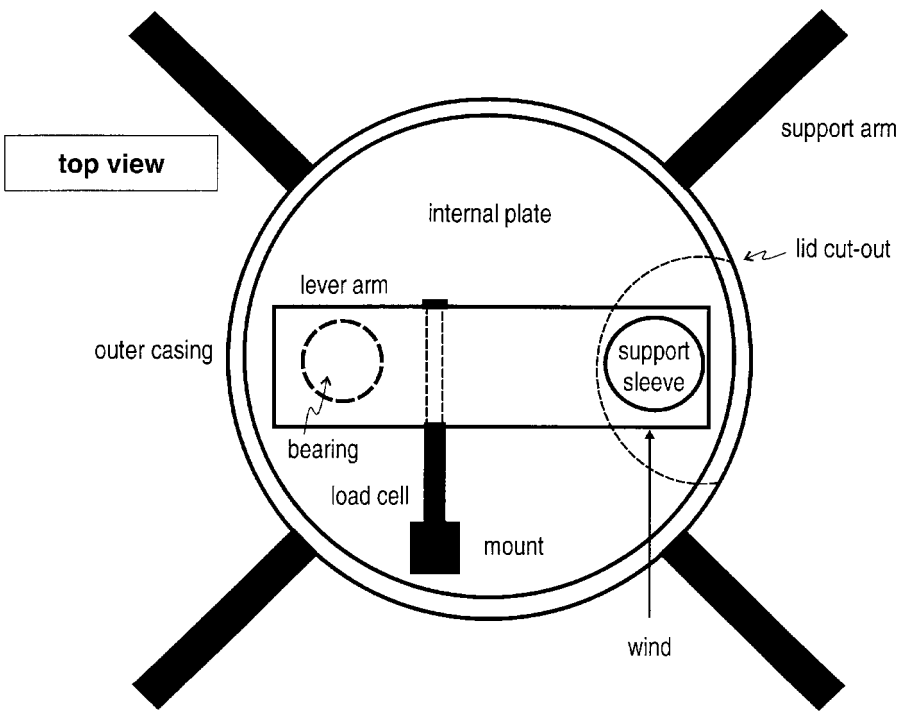

Figure 2. The drag meter design in plan view and in cross-section

firmly into place with the six screws. The roughness element stood upright in the unit. The orientation of the lever arm could be adjusted by loosening the bolt at the base of the internal plate and rotating the plate on the four teflon blocks so as to orient the lever arm perpendicular to the wind direction. When the wind blew against the element, the force applied was transferred down the lever arm. In order to allow the lever arm to swing freely, while resisting warping from torsional stress, a low-friction yet strong bearing was required. A rear-wheel car bearing was used to assure that the measures of momentum would not be lost due to torsion within the instrument; presumably it was strong enough to withstand the 10 kg load of the element since it could support one-quarter of the weight of a car. Likewise, the 101·6 × 50·8 mm, 6·4 mm walled, square aluminum pipe used for the arm had sufficient strength to resist torsion for the element used.

In order to measure the force applied to the element, a load cell was mounted on the 25·4 × 25·4 cm solid aluminium mount, which was bolted to the base of the internal plate, and attached to the lever arm (Figure 2). A sensitive load cell (Durham Instruments, Model LC-18-50, 0–20 kg) was attached to the lever arm and base plate to provide 2 : 1 mechanical advantage to enhance small wind loads.

Once assembled, calibration of the unit was necessary to couple the measured load cell output with the applied force. Under these controlled conditions, the instrument precision was quite high ($r^2 = 0{\cdot}99$, standard error = 0·015 kg). In subsequent calibration test a 10 kg plate was placed on top of the sleeve to determine the effect of placing additional weight on the arm (e.g. a roughness element). No measurable differences were found between weighted and unweighted calibrations.

Field installation of the instrument consisted of digging a hole sufficiently large to house the instrument up to the support arms. Once placed in the hole, the unit was levelled and soil packed around its edges to hold it in place. To measure the applied wind load, the offset value of the load cell was recorded, and the lever arm oriented perpendicular to the wind. The roughness element was then placed in the support sleeve to present the roughness element to the wind as if it were mounted on the surface. Drag data were obtained with a Campbell datalogger at 1 second acquisition intervals with 1 minute averages.

Wind Speed

Measurements of wind speed were made with R.M.Young Rotating Three-cup Wind Sentry Anemometers (model 03001). Wind speeds were obtained from a 4 m tall tower, with anemometers located at heights of 0·35 m, 0·9 m, 1·45 m, 2·00 m, 2·50 m and 4·00 m, located 10 m due south of the experimental tree. Wind direction was measured at a height of 4 m with an electrical resistance wind vane (R.M.Young Wind Sentry, Model 03000). Given the requirement that the lever arm must be perpendicular to the wind, a short wind-speed data acquisition interval of 1 second with 1 minute averages was used. During data acquisition, the wind direction was monitored carefully and if shifts of more than $\pm 20^\circ$ in wind direction were observed the run was aborted. In addition measurements were not made on highly gusty days. Wind-speed data of < 2 m s^{-1} were discarded in that this represents the anemometer stall speeds. The wind speed at the top of the shrub (1·45 m) was used for the determination of the drag coefficient as suggested by Raupach (1992).

RESULTS AND DISCUSSION

Porosity

Figures 3a–c show the three tree configurations used in the study. Optical porosities ranged from 0·19–0·40. As would be expected volumetric porosities were somewhat higher and ranged from 0·55–0·74 (Table I).

Table I. Results of the porosity analysis

Element	Optical porosity	Volumetric porosity
Solid	0·00	0·00
Least porous	0·19	0·55
Medium porous	0·32	0·65
Most porous	0·40	0·74

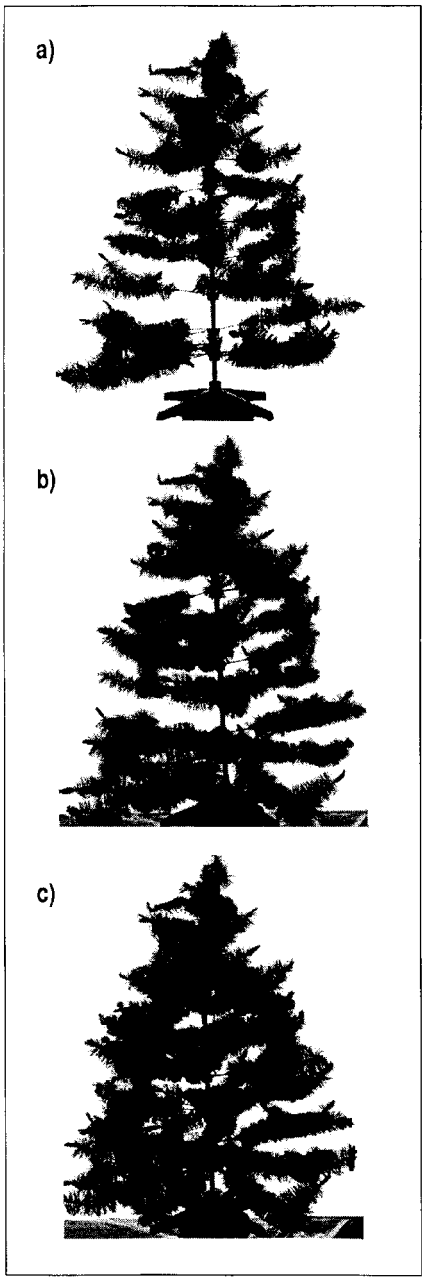

Figure 3. The various shrub porosities and structures used in the analysis. The optical and volumetric porosities are: for shrub a) 0·19 and 0·55, for shrub b) 0·32 and 0·65 and for shrub c) 0·40 and 0·74, respectively

One difficulty with using optical porosity is that two elements of similar optical porosities may have significantly different amounts of pore space within them, altering the way in which the wind would interact with these elements. For example, if the elements in a shrub are distributed over a longer downwind distance the optical porosity may remain at a constant whereas the volumetric porosity will increase.

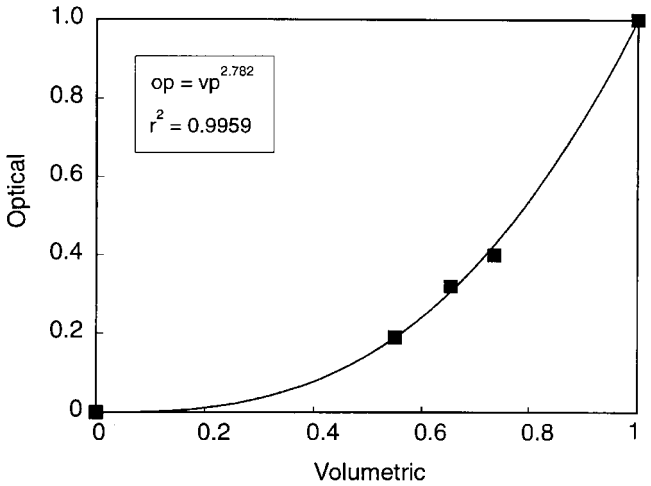

Figure 4. The relationship between volumetric and optical porosity for the shrub studied

As can be seen in Figure 4, optical porosity increases as a power function of volumetric porosity. This relationship can be described by:

$$op = vp^{2.782} \tag{2}$$

Where *op* is the optical porosity and *vp* is the volumetric porosity.

This function fits the data well with a coefficient of determination (r^2) of 0·9959, and meets the physical requirements that for a solid element the model should predict a porosity of 0 and, in the absence of an element, optical and volumetric porosities of 1. The exponent may change not only for a different leaf structure, but also for an element possessing a different depth to width ratio (the depth to width ratio used here is 1 : 1 for all cases). However, the mathematical model of Wang and Takle (1996) predicted that the total drag force of the shelter belt varied only minimally as width was altered.

Drag on Porous Roughness Elements

The range of wind speeds observed yielded data over a Reynolds (R_e) range of $1{\cdot}0 \times 10^4$ to $2{\cdot}5 \times 10^4$. These are plotted against C_d in Figure 5. Also included in Figure 5 are the drag coefficients for a solid cone and cylinder as measured in the field as well as the C_d of 0·6 suggested for porous shrubs by Raupach (1992) and Raupach *et al.* (1993). This C_d value of 0·6 was taken from Taylor's (1988) collection of drag coefficients for surface-mounted solid elements. As can be seen in Figure 5, this C_d value of 0·6 falls within the range of the measured C_d on the solid elements, but the porous elements have higher drag coefficients at all porosities. As the wind speed is increased, increasing the Reynolds number, the drag coefficients for each of the elements decrease.

Figure 6 shows changes of drag coefficient with optical and volumetric porosity for high and low Reynolds numbers. As optical porosity is increased from 0 to 1, the C_d rises initially, peaks at an intermediate value and then drops until a porosity of 1 is reached where C_d equals 0. The curves for volumetric porosity show a similar pattern of change in C_d. The C_d for volumetric porosity rises more slowly, with a peak at an intermediate value and falls as porosity ranges from 0·6 to 1.

As seen in Figure 6, the drag coefficient curves for high and low Reynolds number values begin to converge as porosity increases. This convergence indicates that the drag coefficient becomes relatively independent of the Reynolds number with increasing porosity. This relationship maybe a manifestation of an increased importance on form drag as the individual components of the tree become isolated and exposed to the force of the wind.

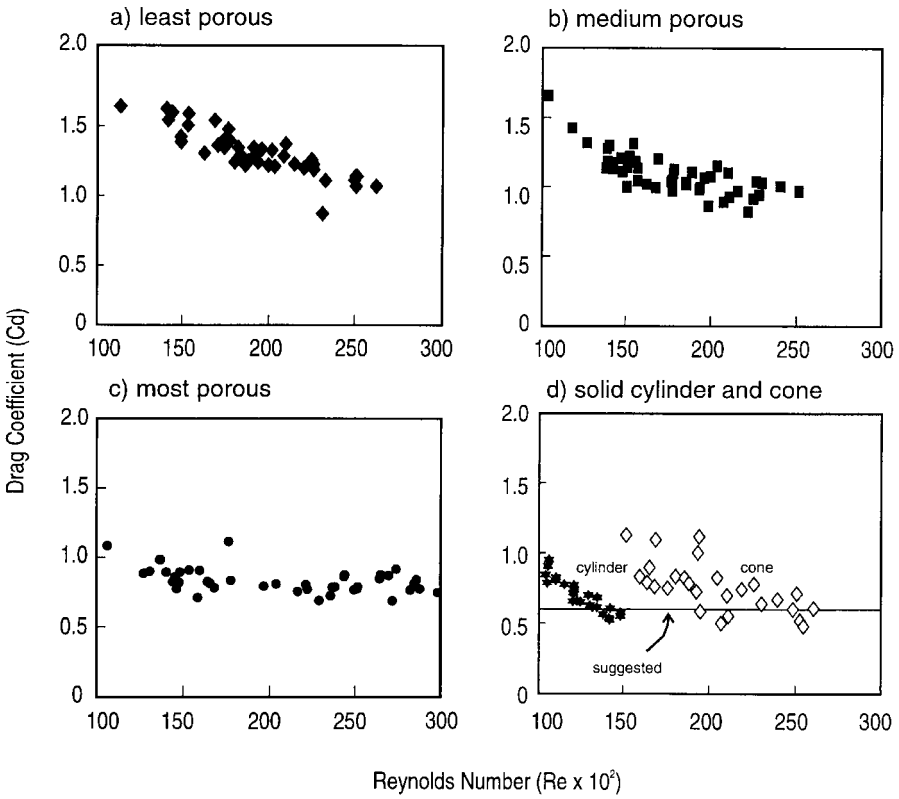

Figure 5. Drag curves for a) the least, b) medium and c) most porous shrub and for d) the cone and cylinder

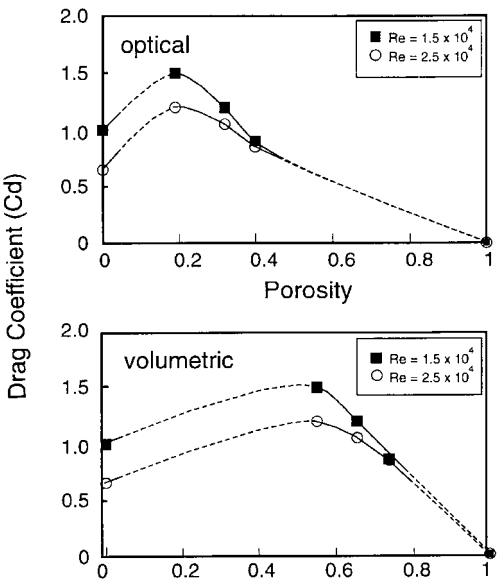

Figure 6. The relationship between optical porosity and C_d and volumetric porosity and C_d

This increased independence of drag coefficient from Reynolds number as porosity increases may be explained by analogy using the concept of flow regimes (see Morris, 1955 or Lee and Soliman, 1977). The solid element can be said to be in a state of truly skimming flow; the wind cannot enter the element but is forced to 'skim' around it. A porous object can be thought of as consisting of a number of individual solid elements (e.g. leaves or leaflets), which interact with one another in a flow similar to wake interference. In this situation some momentum would be extracted by an upwind element (leaf), more by the next downstream element, and so on, until either all of the momentum is extracted or the other side of the shrub is reached. The result would be a higher drag coefficient than for the solid due to the wind interaction with multiple bluff bodies along a single path of flow. As the porosity increases, some of the wakes will no longer interfere with others and a growing portion of the wind would be able to pass through the shrub without a loss of momentum, resulting in a lower drag coefficient. This occurrence is akin to the transition from wake interference flow to an isolated roughness flow and is marked by the peak in the measured drag coefficient of the tree.

IMPLICATIONS AND SIGNIFICANCE OF THE RESULTS

The instrument is simple in design and can be modified for field use on trees within shelterbelts or sites with sparsely arrayed vegetation. Direct measurement of shelterbelt drag coefficient in the field, as opposed to measurements from wind-tunnel or flow field studies, enhances our understanding of the physical mechanisms of the process, thereby increasing the effectiveness and efficiency of our modelling and therefore management capabilities.

The C_d value of 0·6 taken from Taylor (1988) for solid surface-mounted elements agrees well with the values of C_d for the cone and cylinder measured in this study (see Figure 5d), implying that the measured drag coefficients are reliable. Possible sources of error may arise from any deviation of the wind from the perpendicular position of the lever arm, resulting in a loss of measured momentum as the function of a cosine curve. At 20°, the maximum deviation allowed for, a 6 per cent loss in the measured drag would result. These potential sources of drag-force measurement error would result in measured results lower than actual, implying that the porous shrub and other elements examined may have slightly higher drag coefficients than measured.

The results of the porosity analysis may suggest a straightforward relationship between optical and volumetric porosity. Although this may be true when examining elements of similar structure, the relationship is a complex function of the structure and the depth of the element (J. D. Iversen, personal communication). Moreover, caution needs to be used when applying optical or volumetric porosity in an analysis. Optical porosity assumes the wind 'sees' what we as observers see, which is clearly not the case. For example, an object of any density with sufficient depth will eventually obscure transmission of light, although wind may flow through the element with minimal resistance. Previous empirical measurements of drag and drag coefficients have been restricted largely to solid elements, or when porosity is considered, to two-dimensional windbreaks. Taylor (1988) presented a curve showing the relationship between C_d and optical porosity for two-dimensional windbreaks (see Figure 1). Unlike the peak in drag coefficient at an intermediate porosity measured for the tree in this study, the drag coefficients for two-dimensional windbreaks have been observed to decrease on a continuum as optical porosity is increased.

Heisler and Dewalle (1988) report that studies of shelterbelts find that medium-porous barriers are the most effective in reducing the mean, near-ground wind speeds for the longest distances. Peak windbreak efficiency corresponds to the intermediate porosity peak in drag coefficient measured in this study. A possibility is that the peak in drag coefficient may be the mechanism for the observed efficiency of the medium-porous barriers. This peak in the drag coefficient vs. porosity curve for three-dimensional elements (Figure 6) has important implications for modelling wind interaction with individual trees and shrubs and shelterbelts, and has not been noted previously in the literature.

ACKNOWLEDGEMENTS

Funding for this work to WGN from the Natural Sciences and Engineering Research Council of Canada is gratefully acknowledged. We would also like to express our appreciation to Compact Sod Farms Ltd of Cambridge, Ontario for the use of the field site, Valerie Wyatt for her assistance in the field and Marie Puddister for the preparation of the figures.

REFERENCES

Brand, D. G. 1987. 'Estimating the surface area of spruce and pine foliage from displaced volume and length', *Canadian Journal of Forest Research*, **17**, 1305–1308.

Gillette, D. and Stockton, P. H. 1989. 'The effect of nonerodible particles on wind erosion of erodible surfaces', *Journal of Geophysical Research*, **94**, 12885–12893.

Grant, R. 1985. 'The influence of the physical attributes of a spruce shoot on momentum transfer', *Agricultural and Forest Meteorology*, **24**, 7–18.

Hagen, L. J. and Skidmore, E. L. 1971. 'Turbulent velocity fluctuations and vertical flow as affected by windbreak porosity', *Transactions of the ASAE*, **14**, 634–637.

Heisler, G. M. and DeWalle, D. R. 1988. International Symposium on windbreak technology, reprinted from *Agriculture, Ecosystems and Environment*, **22–23**, 41–69. Elsevier Science Publishers BV, Amsterdam.

Hyers, A. D. and Marcus, M. G. 1981. 'Land use and desert dust hazards in central Arizona', *Geological Society of America*, Special Paper **186**, 267–280.

Iversen, J. D., Wang, W. P., Rasmussen, K. R., Mikkelsen, H. E. and Leach, R. N. 1991. 'Roughness element effect on local and universal saltation transport', *Acta Mechanica*, Supplement **2**, 65–75.

Lee, B. E. and Soliman, B. F. 1977. 'An investigation of the forces on three dimensional bluff bodies in rough wall turbulent boundary layers', *Transactions of the ASME, Journal of Fluids Engineering*, **99**, 503–510.

Marshall, J. K. 1971. 'Drag measurements in roughness arrays of varying density and distribution', *Agricultural Meteorology*, **8**, 269–292.

Mayhead, G. J. 1973. 'Some drag coefficients for British trees derived from wind tunnel studies', *Agricultural Meteorology*, **12**, 169–184.

Morris, H. M. 1955. 'Flow in rough conduits', *Transactions of the ASAE*, **120**, 373–398.

Musick, H. B. and Gillette, D. A. 1990. 'Field evaluation of relationships between a vegetation structural parameter and sheltering against wind erosion', *Land Degradation & Rehabilitation*, **2**, 87–94.

Nickling, W. G. and McKenna Neuman, C. 1995. 'Development of deflation lag surfaces', *Sedimentology*, **42**, 403–414.

Raupach, M. R. 1992. 'Drag and drag partition on rough surfaces', *Boundary-Layer Meteorology*, **60**, 375–395.

Raupach, R. A., Gillette, D. A. and Leys, J. F. 1993. 'The effect of roughness elements on wind erosion thresholds', *Journal of Geophysical Research*, **98**(D2), 3023–3029.

Seginer, I. 1972. 'Windbreak drag calculated from the horizontal velocity profile', *Boundary-Layer Meteorology*, **3**, 87–97.

Seginer, I. and Sagi, R. 1971/1972. 'Drag on a windbreak in two-dimensional flow', *Agricultural Meteorology*, **9**, 323–333.

Stockton, P. H. and Gillette, D. A. 1990. 'Field measurement of the sheltering effect of vegetation on erodible land surfaces', *Land Degradation and Rehabilitation*, **2**, 77–85.

Taylor, P. A. 1988. Turbulent wakes in the boundary layer, pp. 270–292 in W. L. Steffen and O. T. Denmead, (eds.), *Flow and Transport in the Natural Environment: Advances and Applications*, Springer-Verlag, Berlin.

Vogel, S. 1989. 'Drag and reconfiguration of broad leaves in high winds', *Journal of Experimental Botany*, **40**, 941–948.

Wang, S. and Takle, E. S. 1995. 'A numerical simulation of boundary-layer flows near shelterbelts', *Boundary-Layer Meteorology*, **75**, 141–173.

Wang, H. and Takle, E. S. 1996. 'On three-dimensionality of shelterbelt structure and its influences on shelter effects', *Boundary-Layer Meteorology*, **79**, 83–105.

Wilson, J. D. 1987. 'On the choice of a windbreak porosity profile', *Boundary-Layer Meteorology*, **38**, 37–49.

Wolfe, S. A. 1993. Sparse vegetation as a surface control on wind erosion, Ph.D. Thesis, University of Guelph, Guelph, Ontario.

Wolfe S. A. and Nickling, W. G. 1996. 'Shear stress partitioning in sparsley vegetated desert canopies', *Earth Surface and Landforms*, **21**, 607–619.

Woodruff, N. P, Fryrear, D. W. and Lyles, L. 1963. 'Engineering similitude and momentum transfer principles applied to shelterbelt studies', *Transactions of the ASAE*, **6**, 41–47.

